applied sciences

MDPI

Article

Performance of Bacterial Concrete with Agro-Waste Capsules

Ivanka Netinger Grubeša [1,*], Dalibor Kramarić [1], Dunja Šamec [2] and Anđelko Crnoja [1]

[1] Department of Construction, University North, 42000 Varaždin, Croatia; dakramaric@unin.hr (D.K.); acrnoja@unin.hr (A.C.)
[2] Department of Food Technology, University North, 48000 Koprivnica, Croatia; dsamec@unin.hr
* Correspondence: inetinger@unin.hr

Abstract

This study investigates the effects of agro-waste-based capsules made from grape seeds and cherry pits on the physical, mechanical, thermal and self-healing properties of concrete. Capsule-containing mixtures were compared with a reference concrete after 28 days of water curing using both standardized and non-standardized testing methods. Capsule incorporation reduced workability by up to 91% and altered air content depending on capsule type, increasing it by 47% for grape seed capsules and decreasing it by 65% for cherry pit capsules. Fresh concrete density was reduced by 5.5% and 6.8% for grape seed and cherry pit capsules, respectively, while hardened concrete density decreased by 11% and 9%, implying lighter structures with improved seismic resistance. Compressive strength decreased by 49% for grape seed capsules and 27% for cherry pit capsules. Thermal conductivity was reduced by 32% and 22%, respectively, indicating improved energy efficiency. Concrete with grape seed capsules showed freeze–thaw performance comparable to the reference concrete after 112 cycles, whereas concrete with cherry pit capsules exhibited superior dynamic modulus behavior, suggesting continuous crack healing, despite significant mass loss due to poor capsule–matrix bonding. SEM analysis showed no significant crack reduction, while EDS revealed calcium-rich areas in grape seed capsule concrete, indicating possible crack healing. Overall, agro-waste capsule concrete shows potential for improving seismic resistance and energy efficiency, although further research is required to clarify the self-healing effect.

Keywords: agro-waste capsules; bacterial concrete; density; compressive strength; thermal conductivity; freeze–thaw resistance; crack healing; SEM/EDS analysis

Check for updates

Academic Editor: Markssuel Teixeira Marvila

Received: 18 December 2025
Revised: 5 January 2026
Accepted: 8 January 2026
Published: 11 January 2026

Copyright: © 2026 by the authors. Licensee MDPI, Basel, Switzerland. This article is an open access article distributed under the terms and conditions of the Creative Commons Attribution (CC BY) license.

1. Introduction

Concrete is the most widely used construction material worldwide; however, its inherent brittleness and low tensile strength make it susceptible to cracking, which significantly compromises durability and service life. Even microcracks can facilitate the ingress of water and aggressive agents, accelerating deterioration processes and increasing maintenance requirements. Conventional repair techniques are often costly, labor-intensive, and environmentally burdensome, thereby motivating the development of autonomous self-healing concrete systems.

Among the proposed self-healing approaches in the literature, bacteria-based self-healing concrete, relying on microbially induced calcium carbonate precipitation (MICP), has emerged as a promising solution. Numerous studies have demonstrated that bacterial incorporation can enhance both fresh and hardened concrete properties, while simultaneously promoting crack healing. Eisa et al. [1] reported that *Sporosarcina pasteurii* and

Rhizobium leguminosarum improve workability, compressive strength, tensile strength, and self-healing capability.

Similar positive effects on mechanical performance have been observed for a wide range of bacterial species, including *Bacillus subtilis*, *B. megaterium*, *B. licheniformis*, *B. sphaericus*, *B. flexus*, and *Sporosarcina koreensis* [2–5]. The improvement of concrete properties through the application of bacteria ranges from minor to very significant levels. For example, Thirupathi et al. [3] identified improvements of up to 7% in compressive strength and up to 17% in tensile strength, while Mohammed et al. [4] reported increases of up to 12% and 9%, respectively. Riad et al. [5] observed improvements of up to 26% in compressive strength and up to 29% in tensile strength, whereas Eisa et al. [1] confirmed exceptionally high increases of up to 98% in compressive strength and up to 137% in tensile strength. The explanation for the increase in mechanical properties using bacteria can be found in the work of Li et al. [6–8]. This group of authors concludes that MICP-induced calcium carbonate precipitation significantly enhances interfacial cohesion in granular systems. Similarly, in concrete it may improve the integrity of the interfacial transition zone between the cement matrix and aggregates or encapsulated particles.

Despite the demonstrated benefits of bacterial incorporation, its effectiveness is highly sensitive to dosage and bacterial activity. Several studies have shown that excessive bacterial dosages do not necessarily improve performance. Vishal et al. [9] demonstrated that lower bacterial concentrations yield higher compressive strength across concretes of different strength classes, while Zaerkabeh et al. [10] identified an optimal optical density of 1.2 for *Sporosarcina pasteurii* to achieve maximum compressive and flexural strength. Similarly, Syed and Pollayi [2] reported that a bacterial content of approximately 10% by cement mass minimizes mass loss due to abrasion and ensures optimal concrete quality. These findings highlight the importance of controlled bacterial incorporation to balance $CaCO_3$ precipitation and matrix integrity.

Beyond strength enhancement, bacterial activity contributes to improved durability by reducing porosity and permeability. Achal et al. [11] and Algaifi et al. [12] demonstrated that $CaCO_3$ precipitation fills pores and microcracks, resulting in increased compressive strength and reduced water absorption. However, these studies also revealed that crack healing is often more effective near the concrete surface than in deeper regions [11,12], indicating limitations related to bacterial activation, nutrient transport, and carrier efficiency.

To enhance bacterial survivability in the highly alkaline cementitious environment, various carrier and encapsulation strategies have been proposed. Lightweight aggregates, expanded perlite, fibers, microcapsules, and hydrogels have been successfully used to protect bacterial spores and enable their activation upon crack formation [13–18]. Zhang et al. [19] observed a gradual reduction in crack width over time in concrete containing *Bacillus cohnii*, confirming the time-dependent nature of bacteria-induced healing. Furthermore, Zhang et al. [20] demonstrated that *Sporosarcina pasteurii* remains effective in alkali-activated concrete when introduced via expanded glass granules, with superior crack healing achieved under wet–dry curing cycles compared to continuous water curing. Safiuddin et al. [21] showed that while individual bacterial species positively influence compressive and splitting tensile strength, combined bacterial systems may negatively affect mechanical performance. In addition, Pei et al. [22] highlighted that bacterial cell walls alone can reduce porosity and enhance compressive strength, emphasizing the complex mechanisms governing bacteria–cement interactions.

With regard to the effectiveness of bacteria in crack healing, the literature indicates that bacterial self-healing concrete can heal cracks with widths of approximately 0.05–0.8 mm. Zhang et al. [19] confirmed effective healing up to 0.05 mm, Mohammed et al. [4] up to 0.2 mm, Achal et al. [11] and Wang et al. [12] up to 0.5 mm, and Khaliq and Ehsan [18]

up to 0.8 mm. However, most authors report that reliable and complete self-healing is generally limited to cracks $\leq$ 0.5 mm, while the healing of wider cracks is partial and highly dependent on curing conditions.

Despite significant progress, the sustainability of commonly used bacterial carriers has received limited attention. Most encapsulation systems rely on synthetic or energy-intensive materials, which partially contradict the environmental objectives of self-healing concrete. Moreover, challenges related to deep crack healing and long-term bacterial viability remain unresolved.

This study addresses these limitations by developing agro-waste-based capsules as sustainable carriers for bacterial self-healing agents in concrete. Agro-waste materials are abundant, low-cost, renewable, and largely underutilized in construction applications. By valorizing agro-waste as an encapsulation medium, the proposed approach integrates bacterial self-healing technology with circular economy principles. Moreover, owing to their lower density compared to conventional concrete constituents, the incorporation of agro-waste materials may reduce the overall weight of reinforced concrete structures and, consequently, enhance their seismic resistance, as structural mass and seismic response are inversely related.

The agro-waste-based capsules are designed to protect bacterial spores during mixing and curing, enable controlled activation upon crack formation and water ingress, and promote effective $CaCO_3$ precipitation within cracks. Compared to conventional carrier systems, this approach offers a dual benefit: enhanced self-healing efficiency and reduced environmental impact through waste utilization and decreased reliance on synthetic materials.

To the authors' knowledge, systematic investigations combining bacterial self-healing concrete with agro-waste-derived encapsulation systems remain scarce. Therefore, this research provides new experimental insights into the physical, mechanical, thermal and crack-healing behavior of concrete incorporating agro-waste-based bacterial capsules, contributing to the development of more sustainable and durable self-healing concrete technologies.

2. Materials and Methods

2.1. Preparation of Self-Healing Capsules Based on Agro-Waste

While *Sporosarcina pasteurii* is the most widely studied bacterium for MICP-based self-healing concrete [6–8,23,24], selected strains of *Bacillus cereus* are alkali-tolerant, form resistant endospores, and can induce calcium carbonate precipitation [25,26]. When appropriately encapsulated, *B. cereus spores* can survive the alkaline cementitious environment and contribute to crack healing, representing a viable alternative with more controlled mineral precipitation.

Bacillus cereus used in this research was isolated from local soil, and a sporulation test was conducted in a liquid sporulation medium with a pH value of 12.5. The medium consisted of a nutrient broth enriched with mineral components required for bacterial spore synthesis. The sporulation test was carried out for one week, after which microscopic slides were prepared and examined under a light microscope. The presence of spores was confirmed, thereby verifying the ability of this bacterium to survive in an alkaline medium. Subsequently, a bacterial bio-calcification test was performed using liquid B4 medium at pH 12.5 over a period of four weeks, confirming the ability of the bacterium to precipitate calcium carbonate.

Furthermore, *Bacillus cereus* bacteria, a broth enriched with mineral substances required for bacterial spore synthesis and distilled water were mixed, and bacterial growth was monitored at temperatures of 24 °C, 30 °C, and 37 °C. Since the most intensive bacterial growth was observed at 37 °C, the bacterial culture was further cultivated at this temperature for 5 days in four bottles, each with a volume of 5 L. After cultivation, a

1 mL subsample was taken from each bottle, and the obtained subsamples were mixed by vortexing for 10 s at 1000 rpm. In the resulting suspension, the total number of bacteria and bacterial spores was determined by a direct microscopic technique in a known sample volume after staining with crystal violet. The total number of bacteria in the medium was 1.4×10^9 per ml of suspension, and the number of spores was 8.1×10^8 per ml of suspension.

For the preparation of self-healing capsules for concrete crack repair, locally available agro-waste (grape seeds and cherry pits) was used, as shown in Figure 1.



Figure 1. Locally available agro-waste in its natural form; grape seeds (**left**) and cherry pits (**right**).

Grape seeds were collected from a winery in eastern Slavonia, Croatia, immediately following the wine production process. Cherry pits were collected from a fruit and vegetable processing facility, also located in eastern Slavonia, Croatia, immediately after cherry processing. Prior to incorporation into the concrete mixture, both grape seeds and cherry pits were subjected to boiling in water for 30 min to suppress germination within the cementitious matrix. The materials were subsequently rinsed with distilled water and dried in a laboratory oven at 70 °C for 24 h.

Seed traits were assessed by measuring bulk density, seed weight, length, and width. Bulk density was determined by filling a 100 mL graduated cylinder with seeds and recording the mass. Measurements were conducted in triplicate. The bulk density was calculated as the ratio of seed mass (g) to the volume occupied in the cylinder (cm^3). Seed weight was measured using an analytical balance (Precisa Gravimetrics AG, Dietikon, Switzerland) by weighing 20 seeds and calculating the average mass per seed (mg). Seed length and width were measured on 20 seeds using a metric ruler with a precision of 0.5 mm and calculating the average value per seed. The water absorption of the seeds/pits was determined in accordance with EN 1097-6 [27]. The test results are presented in Table 1.

Table 1. Characteristics of agro-waste.

Property/Agro-Waste Type	Grape Seed	Cherry Pit
Bulk density (g/cm^3)	0.62 ± 0.01	0.48 ± 0.01
Weight per seed (mg)	27.97 ± 0.46	219.74 ± 0.32
Seed length (mm)	6.0 ± 0.4	8.6 ± 0.7
Seed width (mm)	3.0 ± 0.4	7.6 ± 0.5
Water absorption (%)	31	24

Grape seeds and cherry pits were immersed in a previously prepared suspension for 24 h at atmospheric pressure, as shown in Figure 2.



Figure 2. Immersion of the pits/seeds in a suspension for absorption.

After 24 h spent in the bacterial solution, the pits/seeds were drained and placed into a previously prepared cement paste. Five grape seeds and five cherry pits saturated with a bacterial suspension were sampled, and bacterial survival on these substrates was examined and confirmed. At the same time, the cement paste was prepared from CEM II-A-LL 42.5R cement produced by Grigolin (Nervesa della Battaglia TV, Italy) a crystalline hydrophilic additive VELOSIT CA 112 produced by VELOSIT GmbH & Co. KG, Horn-Bad Meinberg, Germany in an amount of 2% by mass of cement, and water in a quantity such that the water to cement ratio was 0.45. The pits/seeds were coated with the prepared paste and then transferred onto sieves (Figure 3) to allow excess cement paste to drain off, after which they were additionally dusted with cement in order to separate them from each other. The cementitious coating was designed to prevent premature leakage of the bacterial suspension from the capsules until crack formation in the concrete, at which point rupture of the cementitious coating/shell enables activation of the bacterial agent. The capsules prepared in this way are shown in Figure 4. The thickness of the cementitious capsule coating ranged from 0.1 to 0.5 mm, as will be shown later in the microscopic images.



Figure 3. Pits/seeds coated with paste on sieves.

2.2. Cement Properties

The cement used was Portland cement, CEM II/A-LL 42.5R (Nervesa della Battaglia TV, Italy). The density of the cement was 3000 kg/m^3, and the Blaine fineness of the cement grind was 245.1 m^2/kg, both determined in accordance with EN 196-6 [28].



(**a**) Capsules made from grape seeds (**b**) Capsules made from cherry pits

Figure 4. Self-healing capsules.

2.3. Aggregate Properties

All concrete mixtures examined in this study were prepared using dolomite aggregate (fractions 0–4 mm, 4–8 mm, and 8–16 mm), whose particle-size distribution was determined according to EN 933-1 [29] and is shown in Figure 5 together with the cumulative sieving curve.

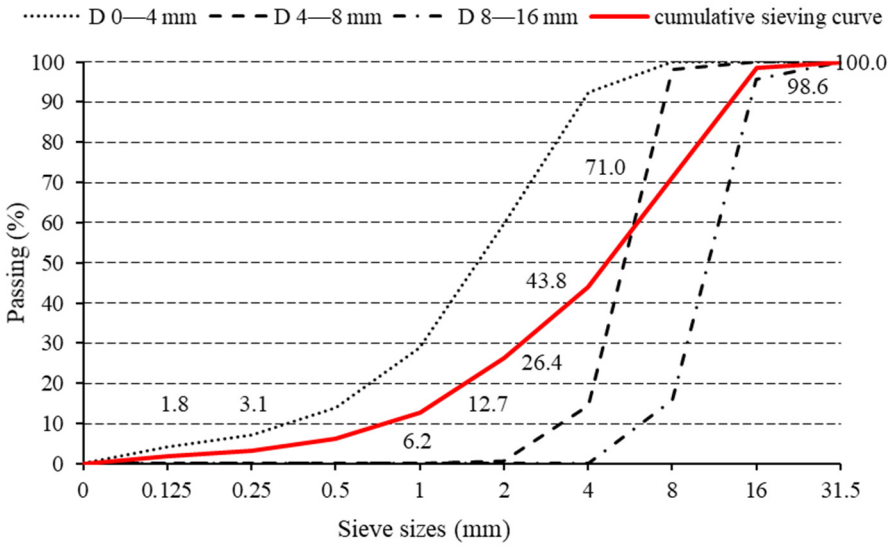


Figure 5. Particle-size distribution of the aggregate.

The aggregate density was 2750 kg/m^3 and the water absorption of dolomite was 1%, both determined in accordance with EN 1097-6 [27]. To prevent water absorption from the concrete during its preparation, all aggregates were pre-saturated prior to incorporation into the concrete—dolomite with water and the capsules with the bacterial solution.

2.4. Properties of Cconcrete Mixtures

Three concrete mixtures (M1, M2, and M3) were prepared, each containing 400 kg of cement, 140 L of water, and 1% superplasticizer by mass of cement. The superplasticizer used was Sika ViscoCrete-4135. The water–cement ratio in all concrete mixtures was 0.35. In the reference mixture, M1, the 0–4 mm aggregate fraction was used in an amount of 845 kg, the 4–8 mm fraction in an amount of 422 kg, and the 8–16 mm fraction in an amount of 653 kg. In mixture M2, 20% of the total aggregate volume was replaced with capsules made of grape seeds, while in mixture M3, 20% of the total aggregate volume was replaced with capsules made of cherry pits. For mixtures M2 and M3, the dolomite aggregate (fractions

0–4 mm, 4–8 mm, and 8–16 mm) was homogenized in a mixer prior to use. Subsequently, 20% of the total volume of the resulting three-fraction aggregate blend was replaced with capsules. Such a high volumetric replacement ratio of aggregate with capsules was selected in order to reduce the density of the concrete and thereby lighten the structure made from this concrete.

In the fresh state, the density of the concrete mixtures was determined in accordance with EN 12350-6 [30], the air content in accordance with EN 12350-7 [31], and the consistency by slump according to EN 12350-2 [32] and by flow test according to EN 12350-5 [33]. The test results are presented in Table 2. Each value represents the mean of three measurements, with a standard deviation of up to 10%.

Table 2. Results of testing fresh concrete mixtures.

Concrete Mixture/Property	M1	M2	M3
Slump consistency (cm)	22	17.5	2
Flow consistency (cm)	61	50	33
Pore content (%)	1.7	2.5	0.6
Density (kg/m^3)	2411	2280	2245

2.5. Specimens Preparation and Testing

From each concrete mixture, twelve cubes with dimensions of 15 × 15 × 15 cm^3 were cast, kept in moulds for 24 h after casting, and subsequently cured by immersion in water for 28 days. After curing, the specimens were divided into four groups and tested as follows:

- Group 1: The density of hardened concrete was determined on three cubes in accordance with EN 12390-7 [34], followed by compressive strength testing according to EN 12390-3 [35].
- Group 2: One specimen measuring 5 × 5 × 3 cm^3 was cut from each of the three cubes (Figure 6). Thermal conductivity was measured using the Hot Disk method, which is based on transient heat transfer principles. A sensor in the form of a thin disk was placed in direct contact with the sample in a so-called "sandwich" configuration. Electrical energy supplied to the sensor produced a heat ultrasonic, generating a transient temperature rise in the sample. Thermal conductivity was calculated from the rate of temperature change. Measurements were performed using a Hot Disk TPS 2500 S instrument (C3 Prozess und Analysentechnik Gmbh, Haar, Germany). The microstructure of the concrete specimens was examined on the same specimens using an optical microscope, with the aim of evaluating the quality of the interfacial transition zone (ITZ) between the aggregate/capsules and the cement paste.
- Group 3: Three cubes were subjected to 112 freeze–thaw cycles in accordance with CEN/TR 15177 [36] (Clause 7) to determine the relative dynamic modulus of elasticity (Clause 7.3.1) and changes in specimen mass during exposure. By subjecting the specimens to freeze–thaw cycles, the aim was to initiate internal cracking within the samples, while the extent of damage and the potential recovery due to the action of self-healing capsules were monitored using a fundamental transverse frequency device.
- Group 4: Cracks were induced in three cubes using a compression testing machine. Specimens with dimensions of 5.5 × 5.5 × 1 cm^3 were then cut from the cracked cubes (Figure 7). These specimens were sprayed with distilled water twice per week for six weeks, and crack widths were measured at two to three locations using SEM. In this way, the intention was to monitor surface cracks, i.e., cracks with widths greater than those induced by freeze–thaw cycling in the specimens of Group 3.



Figure 6. Specimens for testing the thermal conductivity coefficient of concrete.

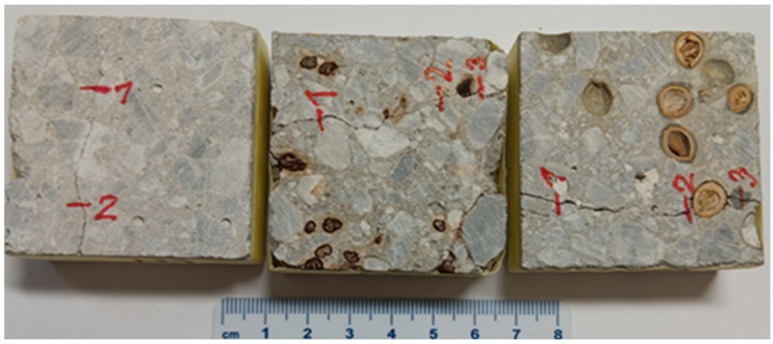
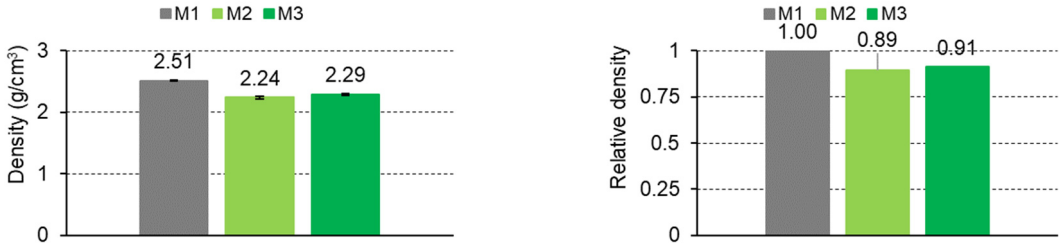


Figure 7. Specimens for monitoring crack width using SEM.

3. Results

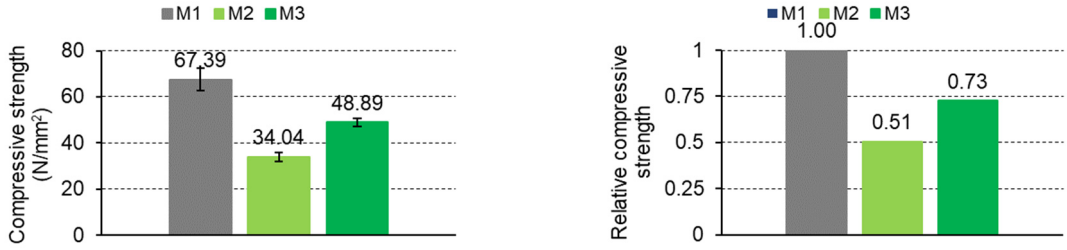
The results of testing the density of hardened concrete are shown in Figure 8a as absolute values and in Figure 8b as relative values, relative to the reference mixture (M1). In the chart showing absolute values, the standard deviation of the measurements is also presented.



(**a**) absolute values (**b**) relative values

Figure 8. Density of concrete in the hardened state.

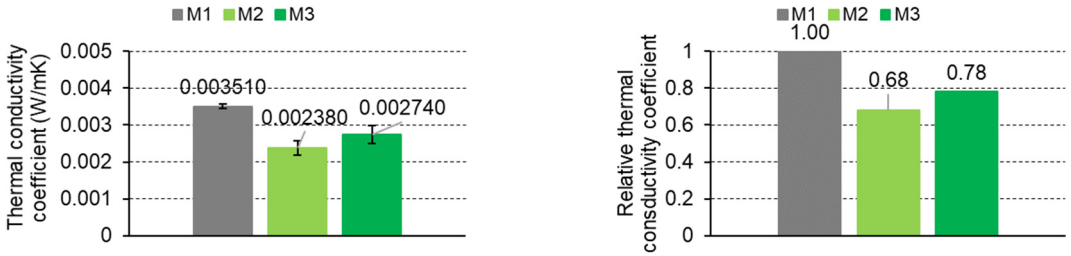
The results of testing the compressive strength of concrete are shown in Figure 9a as absolute values and in Figure 9b as relative values, relative to the reference mixture (M1). In the chart showing absolute values, the standard deviation of the measurements is also presented.



(**a**) absolute values (**b**) relative values

Figure 9. Compressive strength of concrete.

The results of testing the thermal conductivity coefficient of concrete are shown in Figure 10a as absolute values and in Figure 10b as relative values, relative to the reference mixture (M1). In the chart showing absolute values, the standard deviation of the measurements is also presented.



(**a**) absolute values (**b**) relative values

Figure 10. Thermal conductivity coefficient of concrete.

The relative dynamic moduli of elasticity during 112 freeze–thaw cycles are shown in Figure 11, and the change in mass after 112 freeze–thaw cycles is shown in Figure 12. Each point on the curves shown represents the mean value of the measurements with a standard deviation not exceeding 10%. Here it should be noted that the detachment of both types of capsules from the cement matrix was observed after the completion of the exposure of the concrete specimens to freeze–thaw cycles.

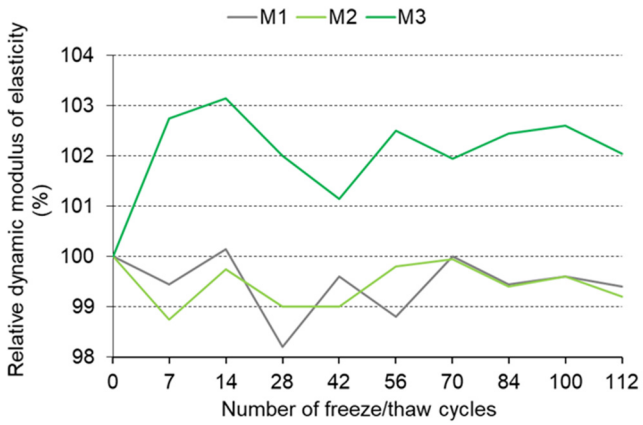


Figure 11. Relative dynamic moduli of elasticity during freeze–thaw cycles.

The results of crack width monitoring by SEM analysis are presented in Table 3. The observed formation of Ca-rich mineral area as well as its chemical analysis is shown in Figure 13. The SEM micrograph presented in Figure 13 was obtained at a magnification of 2000×.

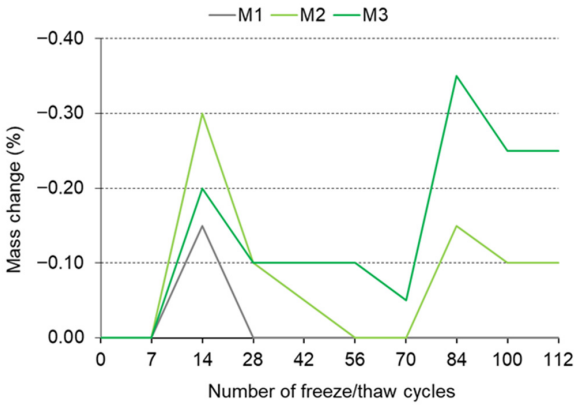


Figure 12. Mass change during freeze–thaw cycles.

Table 3. Results of crack width monitoring using SEM.

Concrete Mixture	Measurement Location	Crack Width Before Treatment (μm)	Crack Width After Treatment (μm)	Reduction (−) /Increase (+) in Crack Width	Observation
M1	Point 1	104.6	107.7	+	-
	Point 2	143.3	143.2	±	
M2	Point 1	241.3	240.7	±	Formation of Ca-rich mineral areas
	Point 2	109.2	109.0	-	
	Point 3	122.9	123.0	±	
M3	Point 1	247.9	240.6	-	Formation of new microcracks
	Point 2	247.9	249.0	+	
	Point 3	98.02	97.65	-	

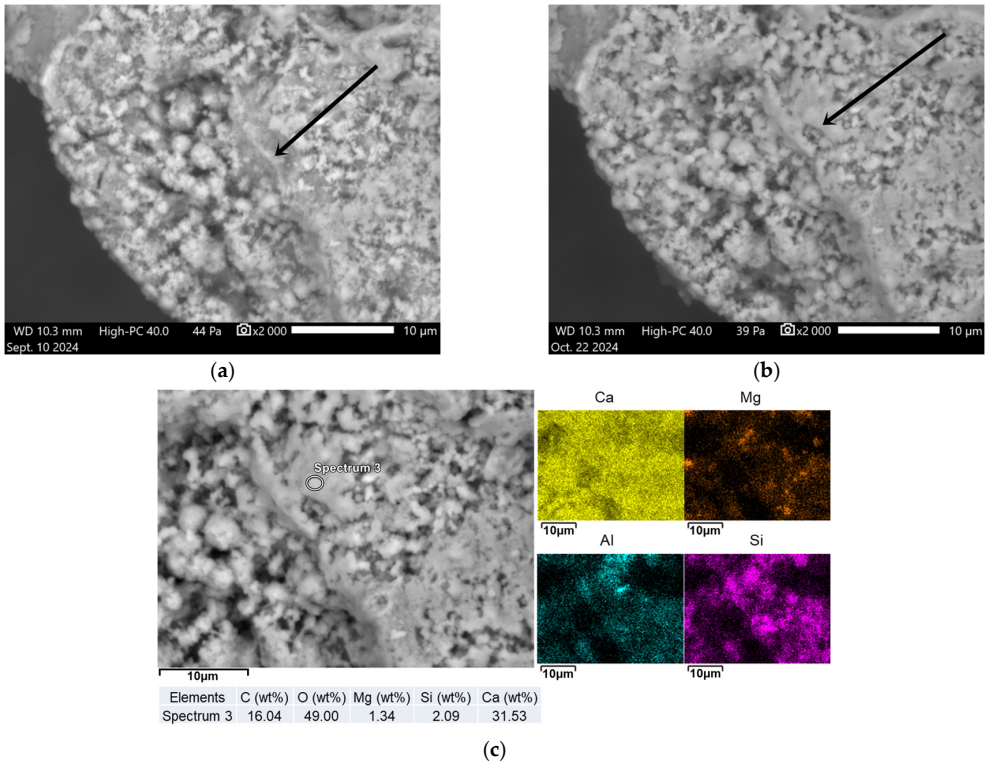
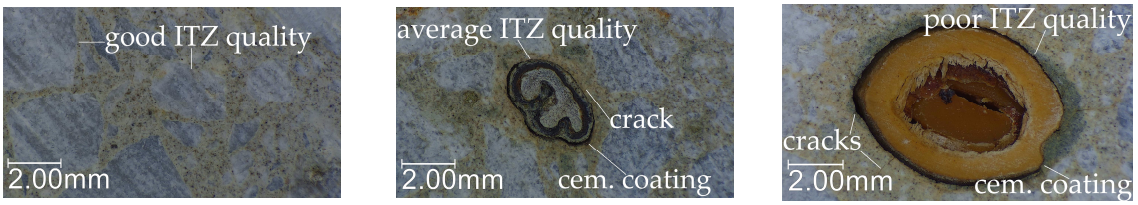


Figure 13. The right side of the crack in the sample M2 (point 3) at the beginning (**a**) and the end of the healing process (**b**). The arrows point out the area of new mineralization, which was analysed by EDXS: elemental mapping and point analysis (**c**).

The appearance of the interfacial transition zone (ITZ) between the aggregate/capsules for all three concrete mixtures is shown in Figure 14.



(**a**) (**b**) (**c**)

Figure 14. Optical microscope images at 50× magnification: (**a**) mixture M1; (**b**) mixture M2; (**c**) mixture M3.

4. Discussion

According to Table 2, both mixtures incorporating capsules exhibit reduced workability compared to the reference mixture (M1). Mixture M2 shows a reduction in workability of 20% relative to M1 when consistency is assessed using the slump test and of 18% when evaluated by the flow table test. A substantially greater decrease in workability is observed for mixture M3, amounting to 91% based on the slump test and 46% based on the flow table test. With regard to pore content, mixtures containing capsules exhibit different trends: the mixture incorporating grape seed capsules (M2) shows an increase in pore content of 47%, whereas the mixture incorporating cherry pit capsules (M3) exhibits a decrease of 65%. The reduced consistency of the capsule-containing mixtures may be attributed to the replacement of 20% of the total aggregate volume, originally consisting of fine and coarse aggregate fractions, with capsules of relatively uniform size. This replacement leads to a reduced proportion of fine aggregate particles, which are known to play a crucial role in concrete workability. The same mechanism may also partly explain the lower pore content observed in mixture M3 compared to mixture M1, as finer aggregate particles are known to introduce a higher pore content in concrete mixtures. In addition, the density of concrete incorporating capsules is reduced in both cases compared to the reference mixture, by 5.5% and 6.8% for grape seed and cherry pit capsules, respectively. This observation is consistent with the lower bulk density of cherry pits compared to grape seeds, as shown in Table 1.

It can be observed from Figure 8a that partial replacement of aggregate with capsules in mixtures M2 and M3 resulted in a reduction in concrete density compared to the reference mixture M1. The mixture containing cherry pit capsules (M3) shows slightly higher density than the mixture containing grape seed capsules (M2); however, both remain significantly lighter than the reference concrete. Figure 8b shows that both capsule-containing mixtures have lower relative density compared to M1. Mixture M2 has a relative density of 0.89, corresponding to an 11% reduction, whereas mixture M3 has a relative density of 0.91, corresponding to a 9% reduction. Comparing M2 and M3, mixture M3 exhibits slightly higher relative density, indicating a somewhat denser structure in concrete with cherry pit capsules than in concrete with grape seed capsules. Replacement of 20% of the aggregate volume with capsules leads to an expected decrease in concrete density. Reducing the weight of structural elements by using lower-density concrete also reduces the overall building mass, which is advantageous in seismically active areas since earthquake-induced inertia forces are proportional to the building mass. The density presented in Figure 8a differs slightly from that reported in Table 2; however, this discrepancy arises from the different states of the material being evaluated. Specifically, Figure 8a reports the density of hardened concrete, whereas Table 2 refers to the density of fresh concrete. According to EN 206 [37], normal-weight concrete is defined by a dry density in the range of 2000–2600 kg/m^3, corresponding to the density shown in Figure 8a. Consequently, all concretes investigated in this study may be classified as normal-weight concretes, despite the relatively high-volume fraction of capsules.

Incorporation of capsules into the concrete matrix significantly reduces compressive strength compared to the reference mixture without capsules (Figure 9a). The compressive strength of concrete containing grape seed capsules (M2) was reduced by 49%, while that of concrete containing cherry pit (M3) capsules was reduced by 27% compared to the reference concrete (Figure 9b). The negative effect is more pronounced for the mixture containing grape seed capsules (M2) than for the mixture containing cherry pit capsules (M3), suggesting that cherry pit capsules have a more favorable mechanical influence on the concrete structure. Comparison of M2 and M3 shows that mixture M3 exhibits approximately 22% higher relative compressive strength than M2 (Figure 9b), confirming that cherry pit capsules cause less reduction in mechanical properties than grape seed capsules. A comparison between mixtures M2 and M3 shows that mixture M3 exhibits approximately 22% higher relative compressive strength than M2 (Figure 9b), indicating that cherry pit capsules result in a smaller reduction in mechanical properties than grape seed capsules. Cherry pit capsules therefore represent a more favorable alternative in terms of maintaining compressive strength. The increase in compressive strength reported in studies [1,3–5] and attributed to bacterial activity could not be clearly identified in the present study, as concrete mixtures containing seeds/pits without bacteria were not included for comparison. Since the minimum required concrete strength class according to EN 1998–1 [38] for the moderate ductility class (DCM) in primary seismic elements is C16/20 and for the high ductility class (DCH) is C20/25, mixtures M2 and M3 are suitable for application in seismically active areas.

Incorporation of capsules into the concrete matrix results in a significant reduction in thermal conductivity (Figure 10a), indicating improved thermal insulation properties. The more pronounced reduction observed in M2 suggests that grape seed capsules have a greater influence on lowering thermal conductivity than cherry pit capsules. Both capsule-containing mixtures show a marked decrease in the thermal conductivity coefficient compared to M1 (Figure 10b). Mixture M2 exhibits a relative value of 0.68, corresponding to a reduction of approximately 32%, while mixture M3 shows a relative value of 0.78, i.e., a 22% reduction compared to M1. Comparison of the mixtures shows that M2 has lower thermal conductivity than M3, meaning that concrete with grape seed capsules exhibits better insulation performance than concrete with cherry pit capsules. These results confirm that the application of capsules reduces concrete thermal conductivity, which is beneficial from the standpoint of thermal insulation. The more pronounced effect observed for M2 indicates a greater contribution of grape seed capsules to improving thermal performance.

Based on the relative dynamic modulus of elasticity during freeze–thaw cycling (Figure 11), the reference mixture M1 exhibits relatively stable performance throughout the test. Values fluctuate slightly without any noticeable degradation trend, indicating good freeze–thaw resistance. Mixture M2 generally exhibits lower relative dynamic modulus values than M1 throughout the test period. A pronounced drop is observed around 28 cycles, where M2 reaches its lowest value. Although partial recovery is reported afterward, M2 mostly remains below the reference curve, indicating lower resistance to freezing and thawing compared to the reference concrete (M1). In contrast, mixture M3 exhibits higher relative dynamic modulus values than M1 throughout nearly the entire testing period. Values generally remain above 101%, with a peak observed after approximately 14 cycles. This indicates that concrete with cherry pit capsules exhibits more favorable behavior under freeze–thaw conditions and greater resistance to damage compared to the reference mixture. Capsule incorporation therefore has variable effects depending on capsule type: grape seed capsules (mixture M2) negatively affect the dynamic modulus of elasticity under freeze–thaw conditions, whereas cherry pit capsules (mixture M3)

exhibit a positive or at least neutral effect, with improved performance relative to the reference concrete.

According to the mass change diagram during freeze–thaw cycles (Figure 12), mixture M1 shows relatively small mass variation. After a slight mass loss of approximately −0.15% at around 14 cycles, values return close to zero by approximately 28 cycles. This behavior indicates good freeze–thaw resistance without significant deterioration. Mixture M2 exhibits more pronounced mass changes compared to M1, with a larger loss at 14 cycles (approximately −0.30%), and continued mass loss during later cycles (around cycles 84–112), maintaining a total loss of approximately −0.10%. This indicates reduced freeze–thaw resistance and probable surface deterioration in M2. Mixture M3 exhibits even less favorable behavior: an early mass loss of approximately −0.20%, followed by a pronounced increase reaching approximately −0.35% at around 84 cycles, and retaining the greatest total mass loss at the end of testing. Compared to M1, mixture M3 demonstrates substantially greater mass degradation, indicating more severe scaling or structural damage during cyclic freezing. In comparison to the reference mixture, M2 shows moderate degradation in freeze–thaw resistance, whereas M3 exhibits the poorest performance with the greatest mass loss. These results indicate that capsules, particularly cherry pit capsules in M3, negatively affect freeze–thaw resistance with regard to mass loss, even though they showed a favorable influence on the dynamic modulus of elasticity in the previous analysis. The reason for the greater mass loss during freeze–thaw cycles in mixtures M2 and M3 can be attributed to the detachment of capsules from the cement matrix, as mentioned in Section 3. The higher mass loss observed in mixture M3 compared to mixture M2 is a consequence of the greater weight of the cherry pits compared to grape seeds, as shown in Table 1.

According to Table 3, no crack healing was observed in mixture M1 during the six-week monitoring period. In mixture M3, a slight reduction in crack width was observed; however, the formation of new cracks was also noted. Mixture M2 exhibited the most favorable response among the investigated mixtures, showing indications of crack width reduction. In terms of their width, these cracks are comparable to those reported by Mohammed et al. [4], which were fully healed; however, this was unfortunately not observed in the present study. However, SEM analysis supported by EDS for mixture M2 revealed the presence of calcium-rich regions (Figure 13), which may be associated with bacterial activity. Specifically, EDS analysis suggested the presence of a $CaCO_3$-rich precipitate with minor amounts of Mg and Si. Deviations from the theoretical $CaCO_3$ stoichiometry are expected due to the semi-quantitative nature of SEM–EDS analysis, particularly for light elements (C and O), as well as potential influences related to sample preparation and interaction volume [39]. Nevertheless, the observed healing effect appears to be limited, and future research will focus on improving healing efficiency through alternative approaches, such as immersion of cracked specimens in water.

Figure 14 illustrates a generally good-quality interfacial transition zone (ITZ) between the dolomite aggregate and the cement matrix in the reference mixture (M1). In mixture M2, a slightly reduced ITZ quality can be observed between the grape seed capsules and the cement matrix, together with occasional cracks extending from the capsules. In mixture M3, the ITZ quality around the cherry pit capsules appears to be poorer, accompanied by a greater number of cracks propagating from the capsules. The thickness of the cement paste layer ranges from approximately 0.1 to 0.5 mm and appears to be more uniform around the cherry pit capsules compared to the grape seed capsules. The cracks observed in the vicinity of the capsules may be related to potential volumetric instability of the seeds/pits. The reduced ITZ quality observed in mixtures M2 and M3 could contribute to capsule detachment from the cement matrix and, consequently, to the mass loss of

concrete specimens during exposure to freeze–thaw cycles. Based on the results presented in Figure 11, it may be suggested that the capsules could play a role in the healing of internal cracks; however, further improvements in their interaction with the cement matrix appear to be necessary.

5. Conclusions

This study examines the effects of agro-waste-based capsules on the physical, mechanical, thermal and self-healing properties of concrete. Concrete mixtures containing capsules produced from grape seeds and cherry pits were compared with a reference mixture. After 28 days of water curing, density, compressive strength, thermal conductivity, freeze–thaw resistance, and crack-healing behavior were evaluated using standardized and non-standardized testing methods. The incorporation of capsules had the following influence on concrete properties:

- Reduced workability by up to 91% and altered the air content depending on the capsule type, increasing it by 47% for capsules with grape seeds and decreasing it by 65% for capsules with cherry pits.
- Both modified mixtures exhibited lower density in the fresh state than the reference concrete, with density reductions of 5.5% for mixtures containing grape seed capsules and 6.8% for those containing cherry pit capsules.
- The density of hardened concrete containing grape seed capsules was reduced by 11%, while that of concrete containing cherry pit capsules was reduced by 9% compared to the reference concrete. This reduced density implies a lighter structure and, consequently, improved seismic resistance.
- The compressive strength of concrete containing grape seed capsules was reduced by 49%, while that of concrete containing cherry pit capsules was reduced by 27% compared to the reference concrete.
- The use of grape seed capsules reduced the thermal conductivity coefficient by 32%, and cherry pit capsules by 22% relative to the reference concrete, which is beneficial in terms of the energy efficiency of structures made with such concrete.
- Concrete containing grape seeds exhibited behavior similar to that of the reference concrete during 112 freeze–thaw cycles, both in terms of the relative dynamic modulus of elasticity and mass loss. Exceptionally good performance during freeze–thaw cycling, with respect to the dynamic modulus of elasticity, was observed for concrete containing cherry pits, indicating continuous healing of cracks formed during freeze–thaw cycles. However, the same concrete exhibited significant mass loss, attributed to the detachment of capsules from the cement matrix due to poor bonding between the capsules and the cement matrix.
- SEM analysis did not reveal a significant reduction in cracking in the concrete samples; however, EDS analysis showed calcium-rich areas in the concrete containing grape seed capsules, which nevertheless suggests crack healing.
- To achieve more pronounced crack healing, alternative curing methods are recommended, such as more frequent spraying of cracks or immersion of cracked concrete in water.
- The use of concrete incorporating agro-waste capsules can improve the seismic resistance and energy efficiency of structures, while further research is required to draw definitive conclusions regarding the self-healing effect.

Future work should focus on improving capsule–matrix bonding, optimizing capsule size distribution and replacement ratios and enhancing healing conditions to improve both durability and self-healing efficiency.

Author Contributions: Conceptualization, I.N.G.; methodology, I.N.G. and D.Š.; formal analysis, I.N.G. and D.Š.; investigation, D.K. and A.C.; resources, I.N.G. and D.Š.; data curation, I.N.G.; writing—original draft preparation, I.N.G., D.K., D.Š. and A.C.; writing—review and editing, I.N.G. and D.Š.; visualization, I.N.G. and D.Š.; supervision, I.N.G.; project administration, I.N.G.; funding acquisition, I.N.G. All authors have read and agreed to the published version of the manuscript.

Funding: This study was conducted within the framework of the "Circular Economy in the Construction Industry" project, funded by University North, Croatia.

Institutional Review Board Statement: Not applicable.

Informed Consent Statement: Not applicable.

Data Availability Statement: The data presented in this study are available on request from the corresponding author.

Conflicts of Interest: The authors declare no conflicts of interest.

References

1. Eisa, A.M.; Tahwia, A.M.; Osman, Y.A.; Elemam, W.E. Characteristics of bacteria-based self-healing rubberized concrete for sustainable and durable construction. *Sci. Rep.* **2025**, *15*, 97174. [CrossRef]
2. Syed, R.; Pollayi, H. Experimental investigation on bacterial concrete using Cantabro loss and UPV. *J. Mech. Behav. Mater.* **2025**, *34*, 20240025. [CrossRef]
3. Thirupathi, S.; Palanisamy, S.; Asokan, V. Enhancing sustainability in construction: Exploring the self-healing mechanisms of bio-concrete. *Res. Eng. Struct. Mater.* **2025**, *11*, 2731–2744. [CrossRef]
4. Mohammed, T.A.; Kasie, Y.M.; Assefa, E.; Getu, Y.M.; Tufa, D.H. Enhancing structural resilience: Microbial-based self-healing in high-strength concrete. *Int. J. Concr. Struct. Mater.* **2024**, *18*, 22. [CrossRef]
5. Riad, I.M.; Amin, M.; Elsakhawy, Y.; Abu El-Hassan, K. Performance study of bacteria on improving fresh, mechanical, and durability characteristics of ultra-high-performance concrete. *Mater. Struct.* **2025**, *58*, 237. [CrossRef]
6. Li, Y.; Li, Y.; Guo, Z.; Xu, Q. Durability of MICP-reinforced calcareous sand in marine environments: Laboratory and field experimental study. *Biogeotechnics* **2023**, *1*, 2. [CrossRef]
7. Li, Y.; Guo, Z.; Wang, L.; Yang, H.; Li, Y.; Zhu, J. An Innovative Eco-friendly Method for Scour Protection around Monopile Foundation. *Appl. Ocean Res.* **2022**, *123*, 103177. [CrossRef]
8. Li, Y.; Guo, Z.; Wang, L.; Zhu, Y.; Rui, S. Field implementation to resist coastal erosion of sandy slope by eco-friendly methods. *Coast. Eng.* **2024**, *189*, 104489. [CrossRef]
9. Vishal, A.; Chepuri, A.; Chandana, N. Assessment of bacteria-based self-healing concrete through experimental investigations—A sustainable approach. *J. Mater. Sci. Mater. Eng.* **2025**, *20*, 15. [CrossRef]
10. Zaerkabeh, R.; Mohammadjafari Sadeghi, A.; Afshin, H.; Majdani, R. Crack healing and mechanical properties of bacteria-based self-healing cement mortar. *Period. Polytech. Civ. Eng.* **2022**, *66*, 581–592. [CrossRef]
11. Achal, V.; Mukerjee, A.; Reddy, M.S. Biogenic treatment improves the durability and remediates the cracks of concrete structures. *Constr. Build. Mater.* **2013**, *48*, 1–5. [CrossRef]
12. Algaifi, H.A.; Abu Bakar, S.; Alyousef, R.; Moh Sam, A.R.; Wan Ibrahim, M.H.; Shahidan, S.; Ibrahim, M.; Salami, B.A. Bio-inspired self-healing of concrete cracks using new B. pseudomycoides species. *J. Mater. Res. Technol.* **2021**, *12*, 967–981. [CrossRef]
13. Lucas, S.S.; Moxhama, C.; Tziviloglou, E.; Jonkers, H. Study of self-healing properties in concrete with bacteria encapsulated in expanded clay. *Sci. Technol. Mater.* **2018**, *30*, 93–98. [CrossRef]
14. Liu, L.; Li, Y.; Song, J.; Zhou, J.; Yi, W.; Ge, Y.; Gao, K. Crack repairing and resistance to water penetration properties of microbial self-healing cement. *Eng. Life Sci.* **2025**, *25*, 70010. [CrossRef] [PubMed]
15. Tie, Y.; Ji, Y.; Zhang, H.; Jing, B.; Zeng, X.; Yang, P. Investigation on the mechanical properties of Bacillus subtilis self-healing concrete. *Heliyon* **2024**, *10*, e34131. [CrossRef] [PubMed]
16. Wang, J.; Dewanckele, J.; Cnudde, V.; Van Vlierberghe, S.; Verstraete, W.; De Belie, N. X-ray computed tomography proof of bacterial-based self-healing in concrete. *Cem. Concr. Compos.* **2014**, *53*, 289–304. [CrossRef]
17. Jiang, L.; Jia, G.; Jiang, C.; Li, Z. Sugar-coated expanded perlite as a bacterial carrier for crack-healing concrete applications. *Constr. Build. Mater.* **2020**, *232*, 117222. [CrossRef]
18. Khaliq, W.; Ehsan, M.B. Crack healing in concrete using various bio-influenced self-healing techniques. *Constr. Build. Mater.* **2016**, *102*, 349–357. [CrossRef]
19. Zhang, J.; Liu, Y.; Feng, T.; Zhou, M.; Zhao, L.; Zhou, A.; Li, Z. Immobilizing bacteria in expanded perlite for crack self-healing in concrete. *Cem. Concr. Compos.* **2022**, *148*, 104873. [CrossRef]

20. Zhang, L.V.; Nehdi, M.L.; Suleiman, A.R.; Allaf, M.M.; Gan, M.; Marani, A.; Tuyan, M. Crack self-healing in bio-green concrete. *Compos. Part B Eng.* **2021**, *227*, 109397. [CrossRef]
21. Safiuddin, M.; Ihtheshaam, S.; Shalam, R.A.K. A study on self-healing concrete. *Mater. Today Proc.* **2022**, *52*, 1175–1181. [CrossRef]
22. Pei, R.; Liu, J.; Wang, S.; Yang, M. Use of bacterial cell walls to improve the mechanical performance of concrete. *Cem. Concr. Compos.* **2013**, *39*, 122–130. [CrossRef]
23. Liu, J.; Xu, H.; Dong, M.; Cheng, Z.; Mi, C.; Sun, S.; Zhu, R.; Han, P. Adaptive Evolution of Sporosarcina pasteurii Enhances Saline–Alkali Resistance for High-Performance Concrete Crack Repair via MICP. *Microorganisms* **2025**, *13*, 1526. [CrossRef]
24. Sowmya, S.; Pannem, R.M.R. Integrating bacteria and fibres for self-healing concrete: A comprehensive review of synergistic effects. *Results Eng.* **2025**, *28*, 107071. [CrossRef]
25. Sohail, M.G.; Al Disi, Z.; Zouari, N.; Al Nuaimi, N.; Kahraman, R.; Gencturk, B.; Rodrigues, D.F.; Yildirim, Y. Bio self-healing concrete using MICP by an indigenous Bacillus cereus strain isolated from Qatari soil. *Constr. Build. Mater.* **2022**, *328*, 126943. [CrossRef]
26. Brasileiro, P.P.F.; Soares da Silva, R.C.F.; Rocha e Silva, F.C.P.; Brandão, Y.B.; Sarubbob, L.A.; Benachour, M. Biomineralization of Calcium Carbonate by Bacillus Cereus for Self-Healing Biocement. *Chem. Eng. Trans.* **2020**, *79*, 97–102. [CrossRef]
27. *EN 1097-6:2013*; Tests for Mechanical and Physical Properties of Aggregates—Part 6: Determination of Particle Density and Water Absorption. CEN: Brussels, Belgium, 2013.
28. *EN 196-6:2019*; Methods of Testing Cement—Part 6: Determination of Fineness. CEN: Brussels, Belgium, 2019.
29. *EN 933-1:2012*; Tests for Geometrical Properties of Aggregates—Part 1: Determination of Particle Size Distribution—Sieving Method. CEN: Brussels, Belgium, 2012.
30. *EN 12350-6:2019*; Testing Fresh Concrete—Part 6: Density. CEN: Brussels, Belgium, 2019.
31. *EN 12350-7:2019*; Testing Fresh Concrete—Part 7: Air Content—Pressure Methods. CEN: Brussels, Belgium, 2019.
32. *EN 12350-2:2019*; Testing Fresh Concrete—Part 2: Slump-Test. CEN: Brussels, Belgium, 2019.
33. *EN 12350-5:2019*; Testing Fresh Concrete—Part 5: Flow Table Test. CEN: Brussels, Belgium, 2019.
34. *EN 12390-7:2019*; Testing Hardened Concrete—Part 7: Density of Hardened Concrete. CEN: Brussels, Belgium, 2019.
35. *EN 12390-3:2019*; Testing Hardened Concrete—Part 3: Compressive Strength of Test Specimens. CEN: Brussels, Belgium, 2019.
36. *CEN/TR 15177:2006*; Testing the Freeze-Thaw Resistance of Concrete—Internal Structural Damage. CEN: Brussels, Belgium, 2006.
37. *EN 206:2021*; Concrete—Specification, Performance, Production and Conformity. CEN: Brussels, Belgium, 2021.
38. *EN 1998–1: 2011*; Eurocode 8: Design of Structures for Earthquake Resistance—Part 1: General Rules, Seismic Actions and Rules for Buildings. CEN: Brussels, Belgium, 2011.
39. Scimeca, M.; Bischetti, S.; Lamsira, H.K.; Bonfiglio, R.; Bonanno, E. Energy Dispersive X-ray (EDX) microanalysis: A powerful tool in biomedical research and diagnosis. *Eur. J. Histochem.* **2018**, *62*, 2841. [CrossRef]

Disclaimer/Publisher's Note: The statements, opinions and data contained in all publications are solely those of the individual author(s) and contributor(s) and not of MDPI and/or the editor(s). MDPI and/or the editor(s) disclaim responsibility for any injury to people or property resulting from any ideas, methods, instructions or products referred to in the content.